LiFi: *The Solution to Radio Frequency Saturation*

Melchi Jatau
Department of Telecommunication Engineering,
Federal University of Technology, Minna,
Minna, Nigeria.
melchi.pg824342@st.futminna.edu.ng

Michael David
Department of Telecommunication Engineering,
Federal University of Technology, Minna,
Minna, Nigeria.
mikeforheaven@futminna.edu.ng

Suleiman Zubair
Department of Telecommunication Engineering,
Federal University of Technology, Minna,
Minna, Nigeria.
zubairman@futminna.edu.ng

2020 International Conference in Mathematics, Computer Engineering and Computer Science (ICMCECS) 978-1-7281-3126-9/20/$31.00 ©2020 IEEE 10.1109/ICMCECS47690.2020.240880

***Abstract*—LED-based lighting is rapidly replacing conventional incandescent and fluorescent lighting due to its high energy efficiency and long usage cycle. Visible Light Communication (VLC) and Light Fidelity (LiFi) have extended this usefulness to the transmission of data, due to LEDs' capability for high rates of intensity modulation. In this paper, we give an overview of the frontend elements and propagation channel of a LiFi Attocell (LAC) Network, and discuss LiFi as an indoor complement to RF communications. MATLAB simulation results are presented to depict the distribution of illuminance and received power in the line-of-sight (LOS) and non-line-of-sight (NLOS) channels. The deterministic channel impulse response (CIR) calculation method is used to obtain our power values. The results show that average received power values of −3.87dBm and 2.28dBm in the downlink channel are possible at standard indoor illumination levels. Based on comparisons with the −83.3dBm received power of user equipment (UEs) at 100m in a 5G system and the properties of radio waves, we show that LiFi can serve as a complementary technology to RF communications and surpass some of its limitations.**

Keywords—VLC, visible light communication, LiFi, light fidelity, 5G, attocell, optical wireless communication.

I. INTRODUCTION

With the significant increase in the number of devices relying on wireless communication, the radio spectrum is becoming increasingly saturated, making it increasingly insufficient for future demands of wireless devices. As of 2017, there were 8.6 billion active mobile connections with an average traffic per device of 2.3 GB per month, and monthly global mobile data traffic is estimated to reach 77 exabytes in 2022, with an annual traffic of around 1 zettabyte [1]. While Wi-Fi continues to make significant strides, with Wi-Fi 6 (802.11ax) having a 25% increase in throughput over Wi-Fi 5 (802.11ac) [2], it is still plagued by the issue of RF saturation. Back in 2014 Wi-Fi traffic accounted for 42% of the global IP traffic [3], and the number of Wi-Fi hotspots is expected to grow from 169 million in 2018 to 628 million by 2023 [4]. Other notable challenges to radio frequency (RF) communication are shadowing due to obstructions, and significant path loss as signals travel over long distances, both of which can be overcome by enhancing the probability of line-of-sight (LOS) by making use of smaller cells [5] [6].

These concerns prompted research into wireless communications using light, known as Visible Light Communication (VLC) [7], on the basis that the visible light spectrum (300—790THz including infrared) is approximately 2,600 times the size of the radio frequency spectrum (3Hz – 300GHz). VLC uses incoherent light, typically from white LEDs, for the dual purpose of lighting and transmission of data across free space. Data to be transmitted is encoded onto the emitted light via intensity modulation (IM) and the data-carrying light is captured via direct detection (DD) at a compatible receiver. It comes with the added advantages of immunity to electromagnetic interference, the lack of licensing (only subject to regulations governing human eye safety), and increased physical layer security due to light's inability to penetrate walls. This makes the use of light for communication necessary in sensitive environments such as hospitals, nuclear plants, and airplanes [5] [8].

Light Fidelity (LiFi) is an extension of VLC which implements bidirectionality, multiuser access and handover capabilities. With its vast license-free spectrum, high data rates, low implementation costs, and the high energy efficiency of LEDs, LiFi is a promising candidate for 5G networks [9]. Infrared radiation is used in the uplink channel for eye safety, though a heterogenous network which uses Wi-Fi for the uplink channel has been proposed [10]. A transmitting LED is known as an optical access point (OAP), and the area covered by the etendue (light cone) of an OAP is known as a LiFi Attocell (LAC). All OAPs in a room are connected by a backhaul, for which Power-over-ethernet (PoE) or powerline communication (PLC) have been proposed, to a central control unit/router and form a LAC network [11]. Walls are typically considered network boundaries.

LiFi was introduced by Professor Harald Haas at TEDGlobal 2011 [12], where he demonstrated seamlessly streaming a high-definition (HD) video over modulated light from an electric lamp. Continued advancements in the field and the development of more efficient LEDs resulted in the introduction of new modulation schemes [13] [14], and achieving increased data rates. In 2012 a data rate of 3.4Gb/s was achieved using a red-green-blue (RGB) LED triplet with wavelength division multiplexing (WDM) [15], and within two years a data rate of 3Gb/s was achieved using only a single blue micro-LED with direct-current biased optical orthogonal frequency division multiplexing (DCO-OFDM) [16]. In 2015, a study suggested data rates in the excess of 100Gbps to be possible [17], when implementing an LED array made up of 12 RGB triplets. In 2019, a data rate of 15.73 Gb/s was achieved using off-the-shelf LEDs worth $0.50, further emphasizing the accessibility of the technology [18].

LiFi is relatively cheap to integrate into everyday use, as it does not require the manufacture of dedicated infrastructure, instead relying on the modification of existing ones. It is

designed to complement RF communication and not replace it, enabling RF base stations to offload users onto available LiFi networks once those users cross into any LAC, thereby freeing RF resources. This makes VLC/LiFi attractive for bridging the global communications divide, and making internet access available to remote areas without adding comparatively significant saturation to the RF Spectrum.

II. Channel Overview

Data to be transmitted is coded and mapped to k M-ary quadrature amplitude modulation (M-QAM) symbols in the frequency domain, which are further grouped into v blocks to form an orthogonal frequency division multiplexing (OFDM) frame [11]. Optical-OFDM (O-OFDM) is a modified form of OFDM used in visible light communication to ensure unipolarity of the signals in the time domain, as light cannot have negative intensities. O-OFDM and its techniques are discussed in [13]. An inverse discrete fourier transform (IDFT) is performed on the OFDM frames, as electrical-to-optical conversion takes place in the time domain. A cyclic prefix (CP) is then added to the start of every O-OFDM frame, to enable inter-symbol interference (ISI) to be mitigated by a tap equalizer at the receiver [19]. Biasing and clipping are then performed on the time domain signal to convert the bi-polar signal to a unipolar signal with a controlled amplitude range, depending on the OFDM technique. This produces clipping noise, which is discussed in [20]. The resulting signal then undergoes electrical-to-optical (E/O) conversion at the LED and is transmitted over a free-space optical channel, during which it experiences co-channel interference (CCI) and picks up additive white gaussian noise (AWGN) before arriving at the receiver. The received signal undergoes the necessary signal processing and recovery to regain the original signal [11].

A. Transmitter

The transmitter in a LiFi system is an LED which generates white light. This can be achieved in one of two ways. The first technique involves the combination of red green and blue (RGB) LEDs to produce white light. The second technique involves using a blue Indium Gallium Nitride (InGaN) emitter that excites a yellow phosphor coating to emit white light. The second technique is more commonly used, and is considered here. Due to the notable delay of the yellow phosphor's re-emission, the modulation bandwidth is limited to approximately 2 MHz [17]. The white LED chips are typically grouped in arrays to create a combined emitter with higher radiant output flux. Since the transmitter serves the dual purpose of illumination and data transmission, the illuminance requirement of the task area determines the transmitted power of the LEDs used. In adherence to the indoor illumination standard and photobiological safety standard [21] [22], the average illuminance for working in the task area, usually 0.75m above ground level, should not be less than 500 lux, though lower light levels may be preferred in residential buildings.

B. Receiver

The receiver frontend is made up of a photodiode, pre-amplifier, an optical concentrator, and an optional optical filter. Received light passes through the optical filter which cuts out background radiation and the slow component from the yellow phosphor emission at the transmitter, and thereby increase the modulation bandwidth to the range of 10–20MHz [10]. The filtered light is converged onto the PD by a collimator lens. The PD converts the received light to an electrical current which is pre-amplified and passed onto signal processing components [11].

C. Propagation Medium

The light emitted from the transmitter travels through free space to arrive at the receiver. A non-directed LOS channel exists between the transmitter and receiver when there is no obstruction between them. A non-directed non-line-of-sight (NLOS) channel exists by default as a result of the reflection of light off surfaces in the room, resulting in frequency-selective fading in the combined channel. The majority of reflections are diffused (e.g. from walls), and as such specular reflections (e.g. from screens and windows) are considered to be special cases [23]. The reflectivity of the walls plays a strong role in NLOS channel performance and building the system's power delay profile, as it is modelled as a secondary distributed light source having an ideal Lambertian radiation intensity pattern ($m = 1$) when modelling the channel.

III. System Model

We make the following assumptions in modelling the channel: the room is a cuboid of dimensions $l_x * l_y * l_z$, and the transmitter is a downlighter placed on the ceiling, with a height equal to the room height l_z. The transmitter and receiver normals are assumed to be perpendicular to the floor plane, with the transmitter oriented downwards and the receiver facing upwards, as receiver alignment has been noted to impact performance [24]. The ray-traced layout of the simulated channel is illustrated in Fig. 1, based on [25].

Equation notation: symbols in bold lowercase ($\boldsymbol{a_s}$) represent vector quantities.

The Euclidean distance D between the transmitter and receiver is given as [11]:

$$D = ||\boldsymbol{a_s} - \boldsymbol{a_r}|| = ((\boldsymbol{a_s} - \boldsymbol{a_r}) \bullet (\boldsymbol{a_s} - \boldsymbol{a_r}))^{1/2}, \quad (1)$$

where $\boldsymbol{a_s}$ *and* $\boldsymbol{a_r}$ are the source and receiver position vectors respectively. The cosines of the angles of emission and incidence are given by:

$$cos(\varphi) = \boldsymbol{o_s}\,(\boldsymbol{a_r} - \boldsymbol{a_s}) / D \quad (2)$$

$$cos(\psi) = \boldsymbol{o_r}\,(\boldsymbol{a_s} - \boldsymbol{a_r}) / D \quad (3)$$

The transmitter LED is assumed to have a Lambertian radiation pattern, which is expressed as [26]:

$$R(\phi_{1/2}) = (m + 1)cos^m(\varphi) / 2\pi \quad (4)$$

Where φ is the radiant angle of LED relative to the receiver, and m is the Lambertian emission order, which corresponds to the directionality of the source and is determined by the half-power semi-angle $\phi_{1/2}$, as [23]:

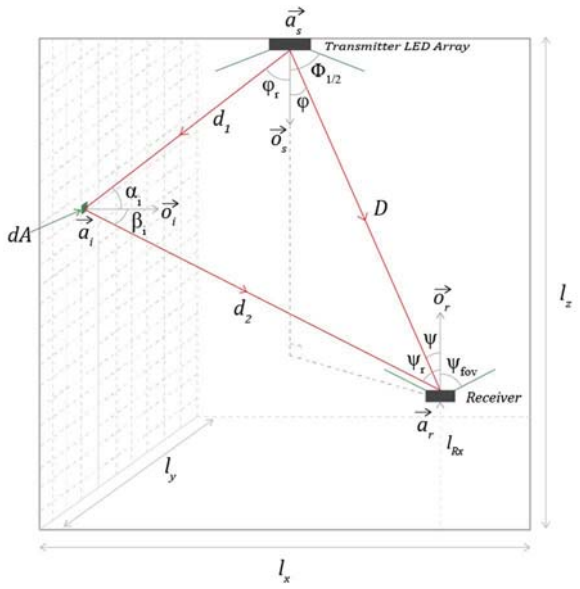

Fig 1. The geometry of the combined channel, based on [25]

$$m = -\ln(5x)/\ln(\cos(\phi_{1/2})) \tag{5}$$

Experiments have shown that the radiation pattern of many typical diffuse-reflector materials present in the NLOS channel such as plaster walls, acoustic-tiled walls, carpets, and unvarnished wood can be well-approximated as Lambertian. Given the area of the receiving photodiode A_{pd}, the solid angle Ω of the radiation from the LED captured by the photodiode is calculated by [11]:

$$\Omega = A_{pd}\cos(\psi) \tag{6}$$

where ψ is the incident angle of the received light.

A. Illuminance

Given a luminous output flux Φ_v, the illuminance from the LOS path at any distance D from the transmitter can be modelled based on (4x) and (6x) by [11]:

$$E_{LOS} = \Omega\Phi_v R(\phi_{1/2}) = \Phi_v\,(m+1)\cos^{(m+1)}(\varphi)/2\pi D^2 \tag{7}$$

where $\cos^{(m+1)}(\varphi)=\cos^m(\varphi)\cos(\psi)$, given that the transmitter and receiver normals are parallel to each other and thus $\varphi = \psi$. As such, the Illuminance vertically below the transmitter at receiver height l_{Rx} can be calculated from (7) as:

$$E_v = \Phi_v A_{pd}(m+1)/2\pi(l_z - l_{Rx}) \tag{8}$$

The illuminance from the NLOS path can be modelled by [27]:

$$E_{NLOS} = \frac{\Phi_v\, dA\, \rho(m+1)\cos^m(\varphi_r)\cos(\alpha_i)\cos(\beta_i)\cos(\psi_r)}{2(\pi d_1 d_2)^2} \tag{9}$$

where ρ is the reflectivity of the material the wall is made of, and dA is the area of a very small partition of the wall the light is incident on.

B. Received Power

Use The LOS channel impulse response of an optical link can be modelled by [25]:

$$H_{LOS} = \frac{A_{pd}(m+1)\cos^m(\varphi)\cos(\psi)G_{fil}G_{con}}{2\pi D^2}, \quad 0\le\psi\le\psi_{FOV} \tag{10}$$

$$H_{LOS} = 0, \qquad \psi>\psi_{FOV}$$

where G_{fil} is the gain of the optical filter, and G_{con} is the gain of the optical concentrator with a field of view ψ_{FOV}, and is calculated as [11]:

$$G_{con} = n^2/\sin^2(\psi_{FOV}), \qquad 0\le\psi\le\psi_{FOV} \tag{11}$$

$$G_{con} = 0, \qquad \psi>\psi_{FOV}$$

where n is the refractive index of the concentrator.

The NLOS channel impulse response for the first reflection can be modelled using the deterministic NLOS CIR calculation method [25]:

$$H_{NLOS}=\frac{A_{pd}(m+1)\rho dA\cos^m(\varphi_r)\cos(\alpha_i)\cos(\beta_i)\cos(\psi_r)G_{fil}G_{con}}{2(\pi d_1 d_2)^2}, \quad 0\le\psi\le\psi_{FOV} \tag{12}$$

$$H_{NLOS} = 0, \qquad \psi>\psi_{FOV}$$

Relative the total optical output power P_t of the source, the received power for the LOS and NLOS channel respectively can be calculated as:

$$P_{r,LOS} = P_t H_{LOS} \tag{13}$$

$$P_{r,NLOS} = P_t H_{NLOS} \tag{14}$$

The total received power can then be obtained as:

$$P_r = P_{r,LOS} + P_{r,NLOS} \tag{15}$$

IV. Simulation Results and Discussion

We evaluate the distribution of illuminance and received absolute power of unmodulated light signals for both the LOS and NLOS channels in a simulation environment, using the deterministic CIR model. The tool used for the simulation is MATLAB R2018b and contour plots under three-dimensional (3D) surface plots were used to generate the resulting figures. Parameters for our simulation are listed in table I. We consider the room's plaster walls to be the only reflecting surfaces for simplicity, and ignore all possible sources of specular reflections.

The result in Fig. 2(a) was obtained using (7) and shows the direct illuminance at receiver height from a single LED array with a cell-center illuminance value of *499.9lux*, which approximately satisfies our illuminance requirement of ≥*500lux*, and an average illuminance value of *154.6lux*. This makes the light source adequate for data transmission while maintaining the illuminance baseline, which results in minimal power consumption and is the basis for selecting it as the transmitter for this study. It should be noted that the illuminance requirement applies to the task area of the room, and not the entire room.

TABLE I. LAC DOWNLINK CHANNEL PARAMETERS

Parameters			Values
Room	Dimensions		(5 * 5 * 3) m
	Reflectivity		0.8
Transmitter	Position(s)	1 LED	(2.5, 2.5)
		4 LEDs	(1.25, 1.25) (1.25, 3.75) (3.75, 1.25) (3.75, 3.75)
	Half-power semi-angle		45º
	Total luminous output flux		5300lm
	Radiant output flux per LED		20mW
	LED Array dimensions		60 * 60
Receiver	FOV		70º
	Area		1cm^2
	Height from ground		0.75m

The illuminance from reflected light (9) is shown in Fig. 2(b), and is observed to contribute an average value of 13.1 lux and a peak value of *24.82lux* at the areas closest to the midpoints of the walls. This is because the beam width ($2\phi_{1/2}$) of the radiation is only wide enough for light to be incident on the lower wall regions closest to the light source, which upon reflection do not travel far from the wall before arriving at receiver height.

Fig. 2(c) shows the LOS illuminance from four sources as would be more likely in a real setting of the given dimensions, using the same LED array. The illuminance is observed to be more widely distributed, and due to the light contribution of other LEDs the cell-center illuminance sees an increase to *675.86lux* with an average value of *505.69lux*. The illuminance from their reflected light is shown in Fig. 2(d), and contributes an average value of *76.32lux* and has a peak value of *105.25lux* at areas around the wall regions having the closest proximity to the light sources, for reasons similar to Fig. 2(b).

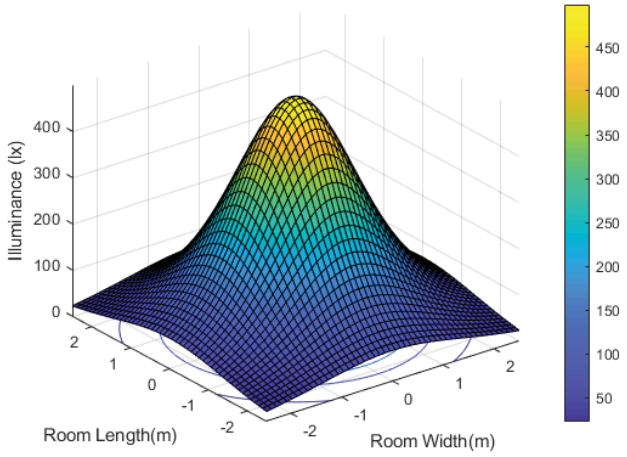

Fig. 2(a) Illuminance distribution for LOS channel from one LED source

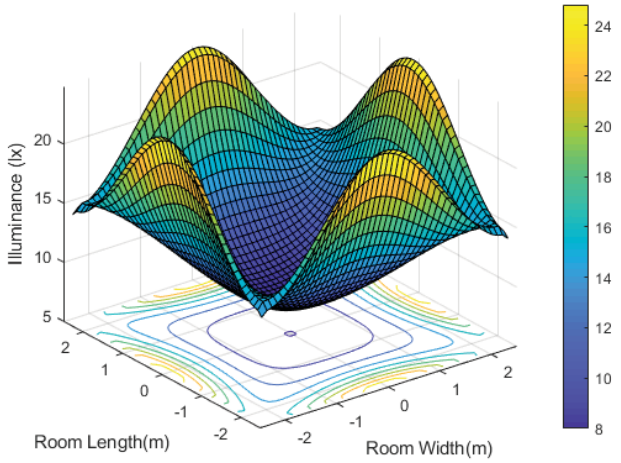

Fig. 2(b) Illuminance distribution for NLOS channel from one LED source

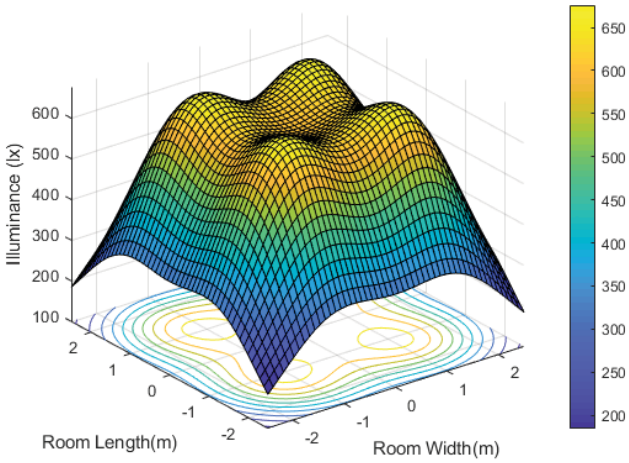

Fig. 2(c) Illuminance distribution for LOS channel from four LED sources

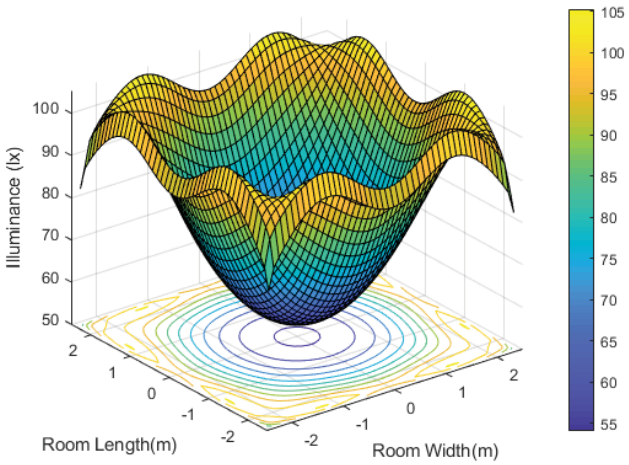

Fig. 2(d) Illuminance distribution for NLOS channel from four LED sources

The result in Fig. 3(a) was obtained using (10) and (13) and shows the LOS absolute power at the receiver in a LAC network with four light sources (OAPs), with a cell-center power value of *3.69dBm (2.34mW)* and average power value of *2.28dBm (1.69mW)*. It is observed that the received power may vary significantly at different regions of the network, falling as low as *−1.95dBm (0.64mW)* at the room corners. A hybrid Wi-Fi/LiFi downlink system has been proposed to enhance user throughput and Quality of Service (QoS) by

taking advantage of the high throughput of LiFi and the ubiquitous coverage of Wi-Fi [5] [28]. An alternative solution is to increase OAP density and implement frequency reuse to reduce the signal-to-interference ratio (SIR) at cell boundaries. Fig. 3(c) shows the case for one LED transmitter.

The reflected power is significantly lower and experiences the widest power differences at different regions of the room, as shown in Fig. 3(b) and Fig. 3(d) and obtained using (12).

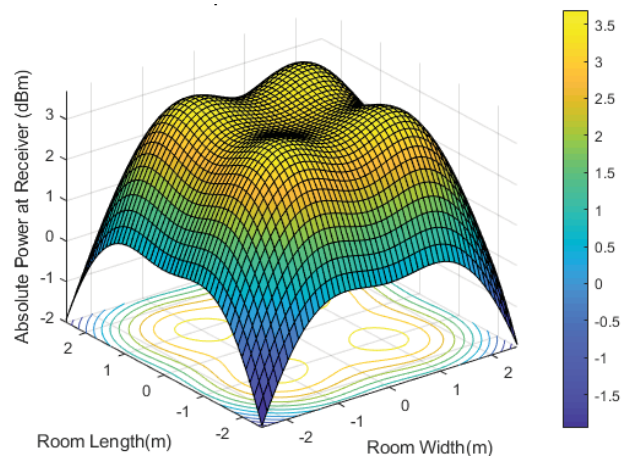

Fig. 3(a) Absolute power received for LOS channel from four LED sources

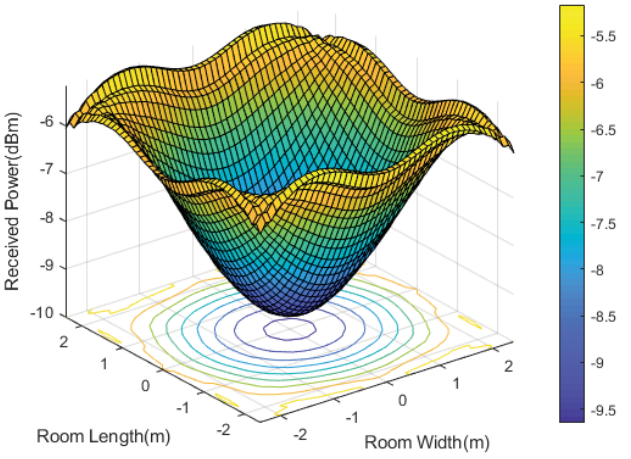

Fig. 3(b) Absolute power received for NLOS channel from four LED sources

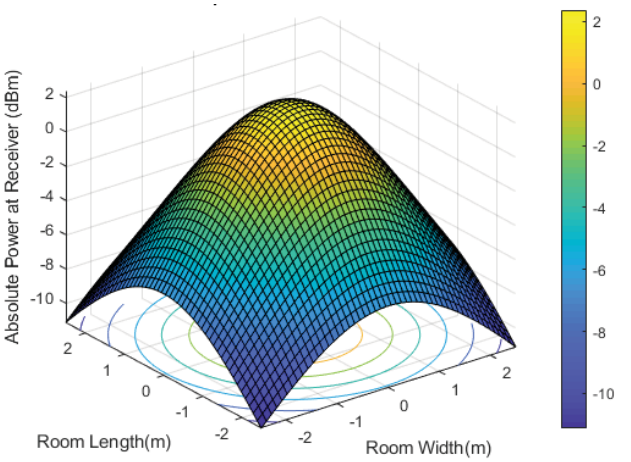

Fig. 3(c) Absolute power received for LOS channel from one LED source

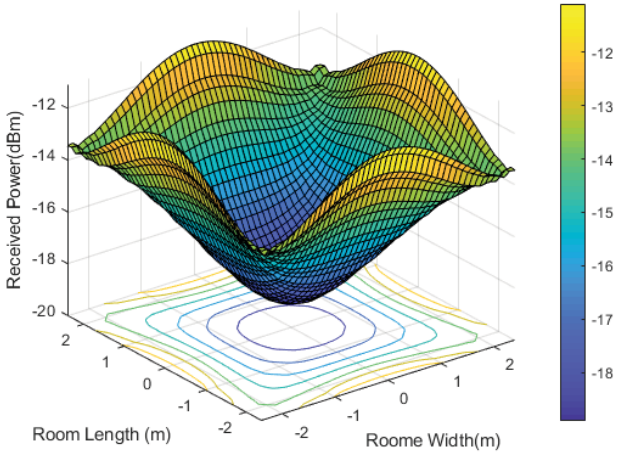

Fig. 3(d) Absolute power received for NLOS channel from one LED source

According to [23], lower power values from reflected paths over multiple reflections yield a larger optical transmission bandwidth. However, this is properly analyzed when considering multiple reflections of light, which is beyond the scope of this study. The complete results obtained are seen in Table II.

V. Conclusion

Channel estimation for the downlink system was performed in this paper by analyzing the illuminance distribution and received power for direct and reflected light with respect to single and multiple phosphor based white LEDs. The illuminance requirement of the space under study was satisfied, and average values for LOS received absolute power -3.87dBm and 2.28dBm were obtained. These sit well above the received signal power of user equipment (UE) in 5G at 100m, measured at *−83.3dBm (4.68nW)* [29]. This is because the highly-LOS nature of LiFi and small cell sizes limit the amount of path loss in the system. The inability of light to penetrate walls also makes possible frequency reuse across multiple LACs without interference, enabling networks to be expanded without consuming more RF bandwidth. Finally, light's ability to be safely used in sensitive environments such as airplanes and nuclear plants

TABLE II. Simulation Results For Illuminance And Received Power

Received Power		**Max value (dBm)**	**Min value (dBm)**	**Average value (dBm)**
LOS	1 LED	2.37	−11.12	−3.87
	4 LEDs	3.69	−1.95	2.28
NLOS	1 LED	−11.09	−46.38	−35.29
	4 LEDs	−5.17	−18.98	−7.37
Illuminance		**(lux)**	**(lux)**	**(lux)**
LOS	1 LED	499.86	22.3	154.6
	4 LEDs	675.86	184.43	505.69
NLOS	1 LED	24.82	7.99	13.1
	4 LEDs	105.25	54.1	76.32

in which radio waves are a potential hazard, enables connectivity to be extended to areas beyond the reach of RF communications with the help of LiFi. Consequently, LiFi stands as a strong candidate to essentially complement RF communications in everyday use.

ACKNOWLEDGMENT

The authors acknowledge the support of the Department of Telecommunication Engineering, Federal University of Technology, Minna, for the foundation of knowledge and access to resources that helped catalyze this research.

REFERENCES

[1] Cisco Visual Networking Index, "Global mobile data traffic forecast update," CISCO, February 2019. [Online]. Available: https://www.cisco.com/c/en/us/solutions/collateral/service-provider/visual-networking-index-vni/white-paper-c11-738429.html.

[2] Wi-Fi Alliance, "Wi-Fi CERTIFIED 6™: A new era in wireless connectivity", 2019. [Online]. Available: https://www.wi-fi.org/downloads-registered-guest/Wi-Fi_CERTIFIED_6_white_paper_20190912.pdf/35680

[3] N. Cheng et al., "A Survey on high efficiency wireless Local Area Networks: Next generation wifi", IEEE Communications Surveys and Tutorials, vol 18, pp. 2315-2344, 2016.

[4] "Cisco annual internet report (2018–2023) white paper", Cisco, February 2020. [Online]. Available: https://www.cisco.com/c/en/us/solutions/collateral/executive-perspectives/annual-internet-report/white-paper-c11-741490.html

[5] H. Haas, L. Yin, Y. Wang and C. Chen, "What is LiFi?," Journal of Lightwave Technology, vol. 34, no. 6, pp. 1533-1544, 2016.

[6] Z. Ma, Z. Zhang, Z. Ding, P. Fan and H. Li, "Key techniques for 5G wireless communications: network architecture, physical layer, and MAC layer perspectives," Science China Information Sciences, vol. 58, no. 4, pp. 1-20, 2015.

[7] T. Komine, M. Nakagawa, "Fundamental analysis for visible-light communication system using LED lights", IEEE Transactions on Consumer Electronics, vol. 50, no. 1, pp. 100-107, 2004.

[8] H. Haas, "LiFi: Conceptions, misconceptions and opportunities," 2016 IEEE Photonics Conference, IPC 2016, pp. 680-681, 2017.

[9] L. Feng, R. Q. Hu, J. Wang, P. Xu, and Y. Qian, "Applying VLC in 5G networks: Architectures and key technologies," IEEE Network, vol. 30, no. 6, pp. 77-83, 2016.

[10] M. Ayyash et al., "Coexistence of Wi-Fi and LiFi toward 5G: Concepts, opportunities, and challenges," IEEE Communications Magazine, vol. 54, no. 2, pp. 64-71, 2016.

[11] H. Haas, C. Chen and D. O'Brien, "A guide to wireless networking by light," Progress in Quantum Electronics, vol. 55, no. June, pp. 88-111, 2017.

[12] H. Haas, "Wireless data from every light bulb," TED, August 2011. [Online]. Available: http://bit.ly/tedvlc.

[13] M. Islim and H. Haas, "Modulation techniques for Li□Fi", ZTE COMMUNICATIONS, vol. 14, pp. 29-40, 2016.

[14] R. Islam, M. Mondal, "Hybrid DCO-OFDM, ACO-OFDM and PAM-DMT for dimmable LiFi", Optik, vol. 180, pp. 939-952, 2019.

[15] G. Cossu, A. Khalid, P. Choudhury, R. Corsini, E. Ciaramella, "3.4 Gbit/s visible optical wireless transmission based on RGB LED", Optics Express, vol. 20, no. 26, pp. B501, 2012.

[16] D. Tsonev et al. "A 3-Gb/s single-LED OFDM-based wireless VLC link using a gallium nitride μ LED", IEEE Photonics Technology Letters, vol. 26, no. 7, pp. 637-640, 2014.

[17] D. Tsonev, S. Videv and H. Haas, "Towards a 100 Gb/s visible light wireless access network," Optics Express, vol. 23, no. 2, pp. 16-27, 2015.

[18] R. Bian, I. Tavakkolnia, H. Haas, "15.73 Gb/s Visible Light Communication with Off-the-Shelf LEDs", Journal of Lightwave Technology, vol. 37, no. 10, pp. 2418-2424, 2019.

[19] D. Tsonev, S. Videv, H. Haas, "Light Fidelity (Li-Fi): Towards All-Optical Networking", Broadband Access Communication Technologies VIII, 2014.

[20] S. Dimitrov, S. Sinanovic, H. Haas, "Clipping noise in OFDM-based optical wireless communication systems", IEEE Transactions on Communications, vol. 60, pp. 1072-1081, 2012.

[21] B. B. Standards, "BS EN 62471:2008," 2008.

[22] E. S. EN12464-1, "Lighting of Indoor Work Places," 2009.

[23] K. Lee, H. Park and J. R. Barry, "Indoor channel characteristics for visible light communications," IEEE Communications Letters, vol. 15, no. 2, pp. 217-219, 2011.

[24] M. D. Soltani, A. A. Purwita, I. Tavakkolnia, H. Haas and M. Safari, "Impact of Device Orientation on Error Performance of LiFi Systems," IEEE Access, vol. 7, pp. 41690-41701, 2019.

[25] M. D. Soltani, X. Wu, M. Safari and H. Haas, "Bidirectional User Throughput Maximization Based on Feedback Reduction in LiFi Networks", IEEE Transactions on Communications, pp. 3172-3186, 2018.

[26] N. Sendani, "Study the Effect of FOV in Visible Light Communication," International Research Journal of Engineering and Technology (IRJET), pp. 759-763, 2017.

[27] Z. Ghassemlooy, W. Popoola, S. Rajbhandari, "Optical Wireless Communications: System and Channel Modelling with MATLAB (Second Edition), 2018.

[28] X. Wu, M. D. Soltani, L. Zhou, M. Safari and H. Haas, "Hybrid LiFi and Wi-Fi networks: A survey", 2020

[29] Huo, Yiming & Dong, Xiaodai & Xu, Wei. (2017). "5G Cellular User Equipment: From Theory to Practical Hardware Design". IEEE Access. 5. 13992-14010. 10.1109/ACCESS.2017.2727550.